IN THE UNITED STATES PATENT AND TRADEMARK OFFICE

In re Application of:	Madhavi Krishnan, *et al.*		
Serial No.:	10/678,805	Group No.:	1637
Filed:	10/3/03	Examiner:	WILDER, Cynthia
Entitled:	**Methods Of Performing Biochemical Reactions Ina Convective Flow Field**		

DECLARATION UNDER 37 C.F.R. §1.132 BY DR. VICTOR M. UGAZ

Commissioner for Patents
P.O. Box 1450
Alexandria, VA 22313-1450

CERTIFICATE OF ELECTRONIC FILING

I hereby certify that this correspondence (along with any referred to as being attached or enclosed) is, on the date shown below, being deposited with the U.S. Patent and Trademark Office, via EFS.

Dated: _ By: _____

Examiner Wilder:

1. I, Victor M. Ugaz, am co-inventor of the claims of the above-referenced application. I am an Associate Professor at the Department of Chemical Engineering, Texas A&M University.

2. I am listed as co-author of Krishnan *et al.*, (2004) "Reactions And Fluidics In Miniaturized Natural Convection Systems," Anal. Chem. 76:6254-6265.

3. Krishnan *et al.* shows that the methods of the instantly claimed invention have the unexpected superior property of yielding about a **10-fold reduction in reaction times** compared to prior art methods. In particular, the ability of one of the invention's embodiments of a closed convective flow thermocycler to perform PCR amplification was compared to a prior art's

conventional thermocycler (T-gradient; Biometra).[1] The data demonstrate "faster reaction speeds (up to **10 times faster)**"[2] when using the invention's convection-driven thermocycling methods compared to the prior art's thermocycler designs.

4. The above-discussed 10-fold reduction in reaction times was **unpredictable, and was empirically determined.**

Dated: 10/7/08 By: Victor M. Ugaz
Dr. Victor M. Ugaz

1 Krishnan *et al.*, page 6259, 1st column, 2nd paragraph.
2 Krishnan *et al.*, page 6265, paragraph bridging 1st and 2nd columns.

Anal. Chem. **2004,** *76,* 6254–6265

Reactions and Fluidics in Miniaturized Natural Convection Systems

Madhavi Krishnan,[†,‡] Nitin Agrawal,[§] Mark A. Burns,[†,∥] and Victor M. Ugaz*[,§]

Department of Chemical Engineering and Department of Biomedical Engineering, The University of Michigan, Ann Arbor, Michigan 48109, and Department of Chemical Engineering, Texas A&M University, College Station, Texas 77843

Buoyancy-driven convection offers a novel and greatly simplified mechanism for generating continuous nonpulsatile flow fields and performing thermally activated biochemical reactions. In this paper, we build on our previous work by constructing a multiwell device incorporating an array of 35-μL cylindrical cavities to perform polymerase chain reaction (PCR) amplification of a 191-base pair fragment associated with membrane channel proteins M1 and M2 of the influenza-A virus in as little as 15 min with performance comparable to conventional thermocyclers. We also describe entirely new adaptations of convective flows by conducting a series of coordinated flow visualization and computational studies to explore the design of closed-loop systems to execute tunable thermocycling, pumping, and mixing operations in a format suitable for integration into miniaturized biochemical analysis systems. Using 15-μL convective flow loops, we are able to perform PCR amplification of the same 191-base pair fragment associated with the influenza-A virus, as well as a 295-base pair segment of the human β-actin gene in a format offering an enhanced degree of control and tunability. These convective flow devices can be further scaled down to nanoliter volumes and are ideally suited as a platform for a new generation of low-power, portable microfluidic DNA analysis systems.

Convective flows are ubiquitous in nature and play a central role in a wide variety of transport processes occurring in the Sun's interior, the Earth's atmosphere and oceans, and industrial processes involving chemical reactions, heat transfer, and crystal growth.[1–6] Of particular interest from both experimental and theoretical standpoints is the case of Rayleigh–Bénard convection, which arises as a consequence of a buoyancy-driven instability occurring when a confined fluid volume is heated from below. The resulting vertical temperature gradient induces an unstable configuration whereby the fluid density at the bottom of the cavity is lower than that of the fluid near the top. The fluid's natural tendency to reorganize in response to this instability, however, is counteracted by the dissipative effects of thermal and viscous diffusion, which must be overcome in order for convective flow to occur. The interplay between these competing processes is characterized by the dimensionless Rayleigh number, *Ra*, which expresses the ratio of buoyant forces driving the instability to diffusive restoring forces acting in opposition.

$$Ra = g\alpha(T_2 - T_1)h^3/\nu\kappa \qquad (1)$$

Here, α is the coefficient of thermal expansion of the fluid, g is the acceleration due to gravity, T_1 and T_2 are the temperatures of the top and bottom surfaces of the cavity, respectively, h is a characteristic length scale (typically the height of the cavity), κ is the thermal diffusivity, and ν is the kinematic viscosity. Despite the relative simplicity of the underlying physics, a multiplicity of beautiful and complex periodic flow patterns can arise under conditions in the vicinity of the onset of convective motion.

Although Rayleigh–Bénard convection has been the subject of intense experimental and theoretical study over the course of the past century, most of this work has focused on flows generated under a narrow range of conditions incorporating (i) low aspect ratio geometries ($h/d \ll 1$, where d is the diameter of the enclosed cylindrical cavity) in which the bounding sidewalls exert a negligible effect on the bulk flow and (ii) extremely small temperature gradients that impose negligible spatial variations in fluid properties within the cavity. Under these conditions, a linear stability analysis can be performed on the momentum and energy conservation equations yielding a critical Rayleigh number for the onset of flow, Ra_{crit}, in the vicinity of 1700.[1]

In the case of high aspect ratio cavities ($h/d > 1$), the situation becomes more complex because the influence of the bounding sidewalls can no longer be ignored.[7–9] If the thermal conductivity

* To whom correspondence should be addressed. Phone: (979) 458-1002. Fax: (979) 845-6446. E-mail: ugaz@tamu.edu.

† Department of Chemical Engineering, The University of Michigan.

‡ Present address: Institut für Biophysik/BioTec, Technical University, Dresden, Germany.

§ Department of Chemical Engineering, Texas A&M University.

∥ Department of Biomedical Engineering, The University of Michigan.

(1) Chandrasekhar, S. *Hydrodynamic and Hydromagnetic Stability*; Clarendon: Oxford, U.K., 1961.

(2) Busse, F. H. *Rep. Prog. Phys.* **1978**, *41*, 1929–1967.

(3) Manneville, P. *Dissipative Structures and Weak Turbulence*; Academic Press: New York, 1990.

(4) Cross, M. C.; Hohenberg, P. C. *Rev. Mod. Phys.* **1993**, *65*, 851–1112.

(5) Getling, A. V. *Rayleigh-Bénard Convection: Structures and Dynamics*; World Scientific Publishing: Singapore, 1998.

(6) Bodenschatz, E.; Pesch, W.; Ahlers, G. *Annu. Rev. Fluid Mech.* **2000**, *32*, 709–778.

(7) Gershuni, G. Z.; Zhukovitskii, E. M. *Convective Stability of Incompressible Fluids (translated from Russian)*; Israel Program for Scientific Translations: Jerusalem, 1976.

(8) Charlson, G. S.; Sani, R. L. *Int. J. Heat Mass Transfer* **1970**, *13*, 1479–1496.

10.1021/ac049323u CCC: $27.50
Published on Web 09/30/2004

of the sidewalls is much greater that of the enclosed fluid, the onset of convective motion scales as $Ra_{crit} = 3450(h/d)$,[4] while a scaling on the order of $Ra_{crit} = 1087(h/d)^4$ is approached for the case of insulating walls. In either case, the most stable critical mode corresponds to nonaxisymmetric fluid motion about the vertical plane of the cavity (i.e., rising in half of the cavity and falling in the other half). The insulating sidewall predictions are consistent with our experimental observations as well as the data of Müller and co-workers, who identified steady and unsteady flow regimes in parameter space defined by the Rayleigh number and aspect ratio for flow of water in cavities up to $h/d = 5$.[10]

In addition to enclosed cavities, buoyancy-driven fluid motion can also occur in closed-loop geometries in response to either vertically or horizontally imposed temperature gradients. The vertical temperature gradient case is often studied in the context of torroidal flow loops in which the upper half of the loop is cooled at a constant temperature while the lower half of the loop is heated with a constant flux. Here, the onset of convective motion generally occurs in the vicinity of $1 < Ra_{crit} < 100$, depending on the details of the geometry and heat-transfer characteristics of the loop.[11] Flows in convection loops can also be generated by horizontal temperature gradients acting orthogonally to the direction of gravitational acceleration. Here, Ra_{crit} depends on both the difference in thermal conductivity between the fluid and the bounding sidewalls and the spacing between the two vertical arms.[7] As in the case of a single vertical cavity, Ra_{crit} is largest in the limit of infinitely conductive walls corresponding to a value on the order of 30 or less where

$$Ra = g\alpha(\Delta T/L)r^4/\nu\kappa \qquad (2)$$

can be defined in terms of the flow channel radius r and horizontal temperature gradient ($\Delta T/L$). This critical value decreases as the sidewalls become less thermally conductive and as the spacing between vertical arms increases.

Recently, we demonstrated a novel device designed to harness the circulatory flow field established by Rayleigh–Bénard convection to perform the temperature cycling necessary to amplify a 295-base pair (bp) segment of the human β-actin gene via the polymerase chain reaction (PCR).[12] This system operates by dispensing a PCR reagent mixture into a high aspect ratio cylindrical cavity whose upper and lower surfaces are maintained at constant temperatures corresponding to annealing/extension and denaturation conditions, respectively. Owing to the nonaxisymmetric nature of convective motion in high aspect ratio systems, the imposed temperature gradient is capable of establishing a circulatory flow pattern within the cavity that continually shuttles reagents through temperature zones associated with denaturation, annealing, and extension reactions, thereby completely eliminating the need for dynamic external temperature control. Furthermore, since the reagents maintain a continual state of thermal equilibrium with their surroundings, convective flow PCR has the potential to achieve rapid cycling times in a format that integrates readily with existing laboratory protocols and liquid handling systems.

A key issue with convection in cavities is that all reagents may not traverse identical paths within the flow field. That is, some fluid elements circulate from the top to the bottom of the cavity, while others traverse paths that may fall slightly short of these temperature extremes. Consequently, critical design parameters such as thermal residence times can only be described in an average sense, integrated over the entire spectrum of flow trajectories. Closed convective flow loops, on the other hand, can be used to generate unidirectional flows along closed paths so that residence times within desired temperature zones can be precisely controlled. Subsequent studies have demonstrated convectively driven PCR in both low aspect ratio cavities using focused infrared heating at the center of the cavity to drive the flow[13] and closed-loop convective flow systems.[14,15]

Ongoing difficulties associated with achieving rapid heating and cooling rates in macroscale thermocycling instruments have motivated recent efforts to investigate the feasibility of performing PCR in microfluidic systems (see for example the recent review by Kricka and Wilding[16] and references therein). These systems typically employ micro- to nanoliter reagent volumes that, by virtue of their small size, can be rapidly heated and cooled. The ability of convectively driven flows to passively establish a steady circulatory flow field within a thermal gradient makes them ideally suited as a novel alternative for performing rapid thermally activated chemical and biochemical reactions like PCR. In this paper, we extend our studies of high aspect ratio cylindrical cavities and investigate harnessing convective flows in closed-loop systems to perform a variety of transport operations associated with microfluidic systems. Using a series of coordinated flow visualization experiments and computational simulations, we show that chip-based convective flow thermocyclers with geometry-dependent control of thermal residence times can be easily constructed. Next, we demonstrate the ability to perform PCR amplification in 15-μL convective loops and show the design and operation of a hybrid polymer–silicon thermocycler incorporating microfabricated heaters to allow direct electronic control of the flow field within the device. We also demonstrate the use of convective flows to achieve velocity-tunable nonpulsatile pumping and droplet mixing in microfluidic channel networks. In each of these applications, the flow can be easily and precisely manipulated by adjusting the magnitude of the applied temperature gradient, the fluidic network geometry, or both. The inherent simplicity and low power consumption of these components make them ideally suited as a platform for a new generation of inexpensive portable chemical and biochemical analysis systems.

EXPERIMENTAL SECTION

Mixing and Thermocycling Studies. A variety of closed-loop microfluidic flow networks were fashioned by an embossing process using melt-processable thermoplastic elastomer substrates.[17,18] First, simple molds were constructed by bending 750-

(9) Charlson, G. S.; Sani, R. L. *Int. J. Heat Mass Transfer* **1971**, *14*, 2157–2160.
(10) Müller, G.; Neumann, G.; Weber, W. *J. Cryst. Growth* **1984**, *70*, 78–93.
(11) Gorman, M.; Widmann, P. J.; Robbins, K. A. *Physica D. Nonlinear Phenomena* **1986**, *19*, 255–267.
(12) Krishnan, M.; Ugaz, V. M.; Burns, M. A. *Science* **2002**, *298*, 793.
(13) Braun, D.; Goddard, N. L.; Libchaber, A. *Phys. Rev. Lett.* **2003**, *91*, 158103.
(14) Chen, Z.; Qian, S.; Abrams, W. R.; Malamud, D.; Bau, H. H. *Anal. Chem.* **2004**, *76*, 3707–3715.
(15) Wheeler, E. K.; Benett, W.; Stratton, P.; Richards, J.; Chen, A.; Christian, A.; Ness, K. D.; Ortega, J.; Li, L. G.; Weisgraber, T. H.; Goodson, K.; Milanovich, F. *Anal. Chem.* **2004**, *76*, 4011–4016.
(16) Kricka, L. J.; Wilding, P. *Anal. Bioanal. Chem.* **2003**, *377*, 820–825.

μm-diameter metallic wire in the shape of the desired channel structures and joining the free ends of the wire loop using epoxy or solder. A 1 cm^2 × 2 mm thick slab of elastomer material was then heated near its melting point (slightly above 100 °C), brought into contact with the wire mold while applying gentle pressure by hand, cooled to room temperature, and released by peeling from the mold. For flow visualization studies, the molded open channels were filled with an aqueous suspension of 6-μm-diameter fluorescent latex microspheres and sealed by placing a second 1-mm-thick elastomer slab on top of the channel network. Sealing was easily accomplished by self-adhesion of the elastomer material at room temperature, creating a stable bond whose strength increased with time and exposure to elevated temperatures. The sealed device was then mounted vertically with the bottom surface in contact with a constant-temperature hot plate, and flow patterns were imaged using a fluorescence microscope.

PCR Studies in Cavity Systems. PCR amplification was performed using home-built cavity-based multiwell devices consisting of interchangeable plastic reaction chamber "cartridges" sandwiched between two aluminum plates: a bottom plate heated with inexpensive cartridge heaters using a microprocessor-driven temperature controller to regulate thermal output and an upper plate whose temperature was regulated with a recirculating water bath. Before loading reagents, the lower surface of the PCR reaction cartridge was sealed using a thin sheet of polycarbonate film bonded by inserting the cartridge into the PCR device and heating briefly to 125 °C. Reagents were then pipetted into the reaction chambers, and the upper surface of the cartridge was sealed with the same adhesive film used to encapsulate conventional PCR multiwell plates. Potential issues associated with trapped air pockets inside the cavities were avoided by slightly overfilling the reactors. An appropriate intercavity spacing was chosen to allow sufficient room for the excess outflow to escape without encountering a neighboring cavity, thereby avoiding cross-contamination issues. The sealed cartridge was then reinserted into the PCR device, which was set to maintain the upper and lower surfaces of the cartridge at their respective reaction temperatures. Preheating the aluminum blocks before inserting the cartridge greatly reduced thermal transients, allowing the convective flow field to attain steady state within 1−2 min. After the reaction proceeded for the desired time, the heaters were switched off and the lower (hot) surface of the device was rapidly cooled by placing it on top of a chilled aluminum block. This protocol allowed the flow (and PCR) to be arrested within a few seconds so that the total reaction time could be accurately controlled. Denaturing and anneal/extend temperatures of 96 and 61 °C, respectively, were used to perform the reaction.

PCR Studies in Loop Systems. The devices used for loop-based PCR were constructed either by using 28-gauge FEP fluoropolymer tubing (Zeus Industrial Products, Inc.) or by drilling channels in Plexiglas blocks, similar to the cavities described in our previous studies.[12] Tubing segments 9 cm in length (15-μL volume) were filled with PCR reagents, and the ends of the tubing were joined with a short segment of lower gauge tubing. Slightly overfilling the loop prior to joining the ends alleviated bubbling problems associated with trapped air pockets. The assembled loop was then wrapped around a triangular-shaped mounting fixture in which opposite arms of the loop were maintained at 95 (denature) and 72 °C (extension) using independently controlled Peltier heaters (Melcor). Aluminum adhesive tape was used to affix the tubing directly to the Peltier surfaces to ensure good thermal contact. The average temperature in the third arm of the loop was passively maintained at 55°C. Using this arrangement, temperatures were measured using thermocouples affixed to the Peltier surface.

Plexiglas devices were constructed by drilling two sets of channels (~900 μm in diameter), each set at right angles to the other, so that they intersected to form a rectangular loop structure in the core of the Plexiglas block (roughly 1 cm × 1 cm × 0.5 cm). Three of the four vents in the structure were blocked by filling with epoxy while the remaining one served as an access point for loading and unloading reagents. The total volume of the loop was 15 μL. Temperature measurements in the denaturing and anneal/extend zones of the loop were performed by inserting a thermocouple into the loop structure prior to sealing the vents. Denaturing and anneal/extend temperatures of 90 and 58 °C, respectively, were used to perform the reaction.

PCR Conditions. PCR amplification in cavity and loop-based devices was demonstrated by amplifying a 191-base region associated with the membrane channel proteins M1 and M2 of the influenza-A virus. Forward and reverse primer sequences were 5′-GCAGCGTAGACGCTTTGTCCAAAAT-3′ and 5′-CAGCCCCC-ATCTGTTGTATA TGAG-3′. Standard 50-μL reaction mixes contained 30 μL of optimized buffer/dNTP mix, 10 μL of primer mix, 8.75 μL of ddH_2O, and 1 μL of template DNA (3.9-kb control sample or dilution of previously amplified 191-bp product) (Maxim Biosciences), and 0.25 μL of 5 units/μL AmpliTaq polymerase (Applied Biosystems). Products were aspirated from the reaction chambers, run on a 2% agarose gel at 60 V for 1 h, and stained with 1× SYBR-Green I. Product yields were measured from purified PCR products (QIAquick PCR Purification Kit; Qiagen) using a NanoDrop ND-1000 spectrophotometer.

PCR amplification in convective flow loops was also demonstrated by amplifying a 295-bp segment of the human β-actin gene (TaqMan PCR kit with β-Actin Detection Reagents; Applied Biosystems). Forward and reverse primer sequences were 5′-TCACCCACAATGTGCCCATCTACGA-3′ and 5′-CAGCGGAAC-CGCTCATTGCCAATGG-3′. Reactions contained 10 mM Tris-HCl, pH 8.3, 50 mM KCl, 3.5 mM $MgCl_2$, 0.2 mM each dATP, dCTP, dGTP, and dUTP, 0.4 ng/μL human DNA, and 0.1 unit/μL AmpliTaq polymerase (Applied Biosystems). The reaction was run for ~30 min, aspirated from the reaction chamber, stained with 10× SYBR-Green I, and run on a 10% polyacrylamide gel at 110 V for 1 h.

Simulations of Convective Flow Patterns. Steady-state flow patterns within the cavities and loop structures were simulated in two dimensions using FLUENT with water as a Boussinesq fluid. Constant-temperature boundary conditions were imposed at the top and bottom surfaces, while a linear temperature gradient in the vertical direction was imposed at the Plexiglas sidewalls.

RESULTS AND DISCUSSION

We present results on mixing, pumping, and thermocycling operations in miniaturized systems using Rayleigh−Bénard convection. Miniaturized systems exploiting such novel fluidic phe-

(17) Sudarsan, A. P.; Ugaz, V. M. *Anal. Chem.* **2004**, *76*, 3229−3235.
(18) Sudarsan, A. P.; Wang, J.; Ugaz, V. M. In preparation.

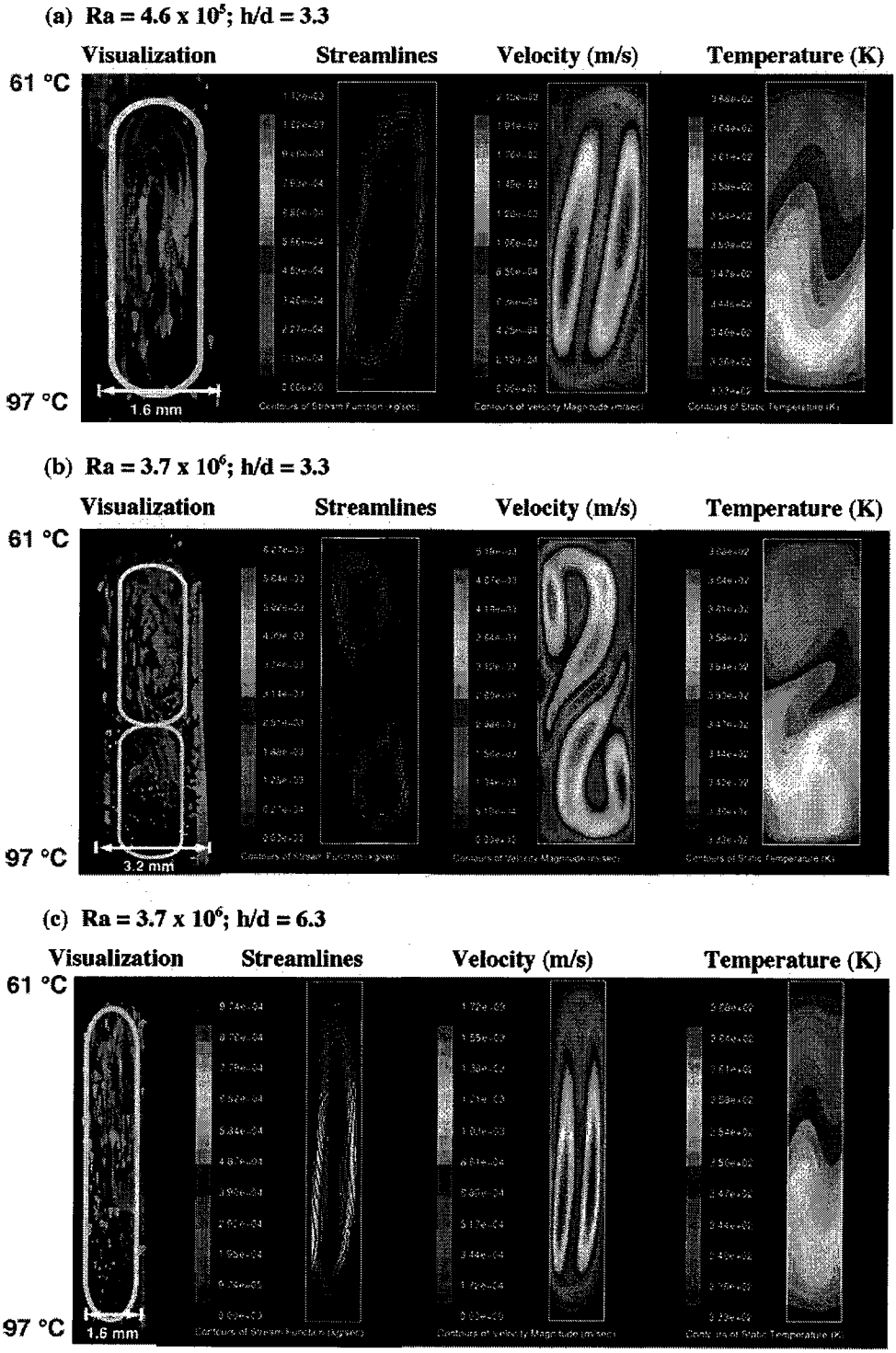

Figure 1. Simulations and flow visualization studies showing the influence of geometry on Rayleigh–Bénard convection in high aspect ratio cavities. (a) $h/d = 3.3$, $Ra = 4.6 \times 10^5$; steady circulatory convective flow between the top and bottom of the cavity. (b) $h/d = 3.3$, $Ra = 3.7 \times 10^6$; unsteady "figure 8" convective flow pattern. (c) $h/d = 6.3$, $Ra = 3.7 \times 10^6$; steady convective flow is reestablished at the same value of Ra as in (b). Rayleigh numbers are computed based on physical properties of water at 80 °C. The particle paths depicted in these images were produced by averaging the recorded fluorescent microsphere trajectories over a time interval of 1 s. Movies of the convective motion in (b) and (c) are available online as Supporting Information.

nomena have the potential to provide precise manipulation of flow fields in a greatly simplified format without the need for intricate fluidic networks, external pumping hardware, and complex electronic control circuitry.

Flow and Thermocycling in Cavity Systems. In a previous paper, we demonstrated DNA amplification in high aspect ratio cavities using Rayleigh–Bénard convection.[12] A temperature gradient was established between the upper and lower surfaces

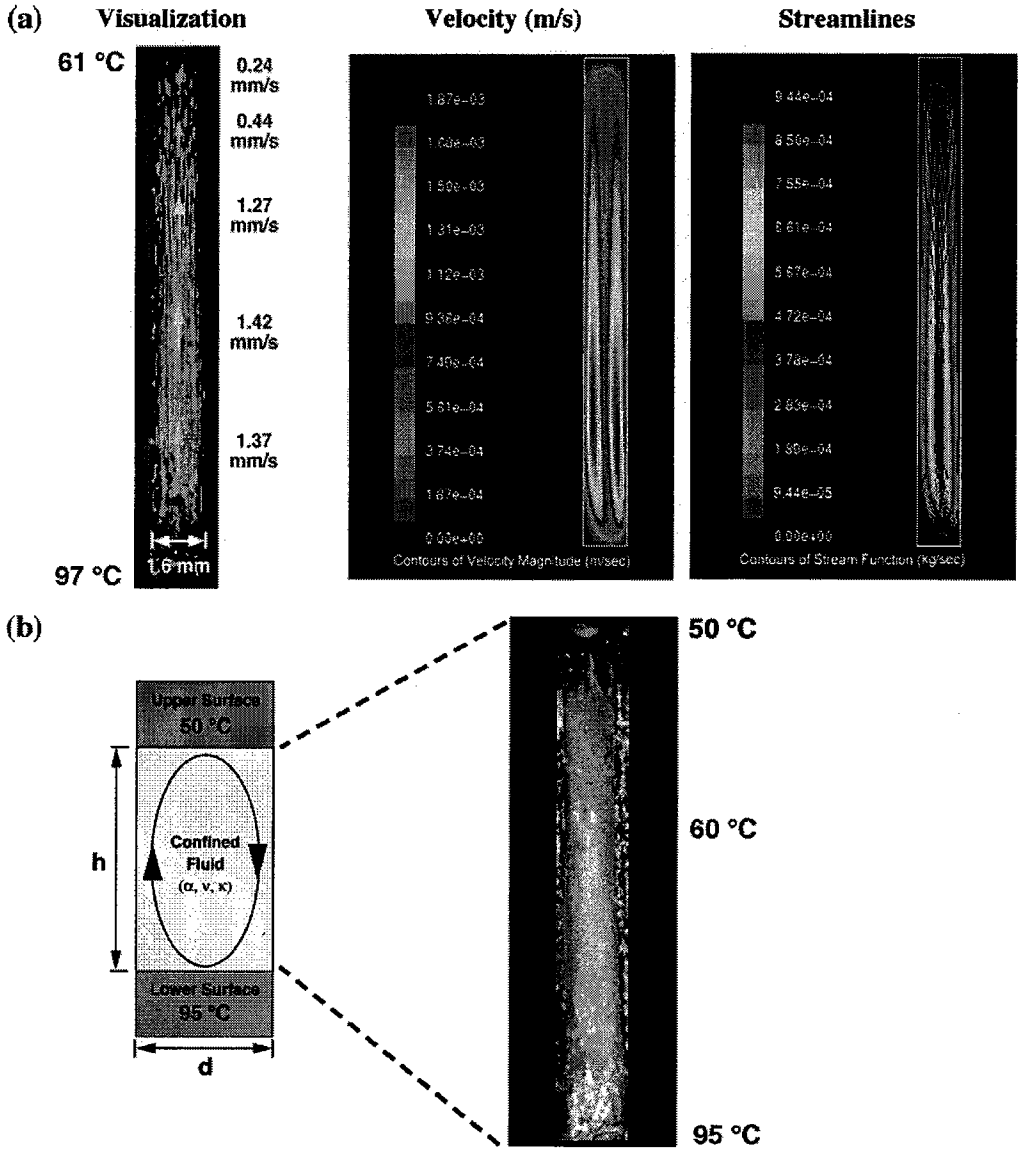

Figure 2. Simulation and visualization of the convective flow field in a high aspect ratio ($h/d = 10$) convective flow cavity. The top and bottom surfaces of the cavity are maintained at $T_1 = 61$ °C and $T_2 = 97$ °C respectively, and $Ra = 1.3 \times 10^7$ (based on physical properties of water at 80 °C). (a) Particle traces showing microsphere displacements over a 4-s time interval. The vertical orientation of the streaks is characteristic of the steady circulatory flow field. Local velocities are indicated by the superimposed vectors, corresponding to values of (i) 0.24, (ii) 0.44, (iii) 1.27, (iv)1.42, and (v) 1.37 mm/s. Velocities were determined by measuring the average length of particle traces formed during a set time interval in the vicinity of the locations depicted in the figure. (b) Experimental verification of the temperature profile within a cavity ($h/d = 10$) using a suspension of thermochromic liquid crystals (blue at 80 °C and above, red at 60 °C, and colorless below 60 °C). A movie of the convective motion and temperature profile in (b) is available online as Supporting Information.

that induced a circulatory flow pattern within the cavity that continually shuttled reagents through temperature zones associated with annealing, extension, and denaturing conditions. We studied flow patterns in a series of these high aspect ratio convection cavities in Plexiglas substrates by recording the motion of an aqueous suspension of 6-μm-diameter fluorescent latex microspheres. The experimentally observed flow patterns are consistent with our flow simulation results indicating that transitions between steady and unsteady motion can be induced by changes in *Ra*, *h/d*, or both (Figure 1). These observations are also in qualitative agreement with the data available in the literature,[10] verifying the reproducibility of the generated flow patterns.

To experimentally verify the temperature profiles in the flow cell, we replaced the solution of fluorescent microspheres in the cavity (h = 15 mm, d =1.5 mm) with a dilute suspension of thermochromic liquid crystals exhibiting a color transition in the range of 60−80 °C (Hallcrest, Inc.). Thermochromic liquid crystals have been widely used to map temperature distributions in a variety of flows.[19] The device was placed on a constant-temperature hot plate such that the bottom of the cavity experienced a temperature of ~95 °C while the top surface of the device was exposed to ambient air and reached a temperature of 50 °C. The observed flow pattern and temperature profile in the cavity are in

(19) Smith, C. R.; Sabatino, D. R.; Praisner, T. J. *Exp. Fluids* **2001**, *30*, 190−201.

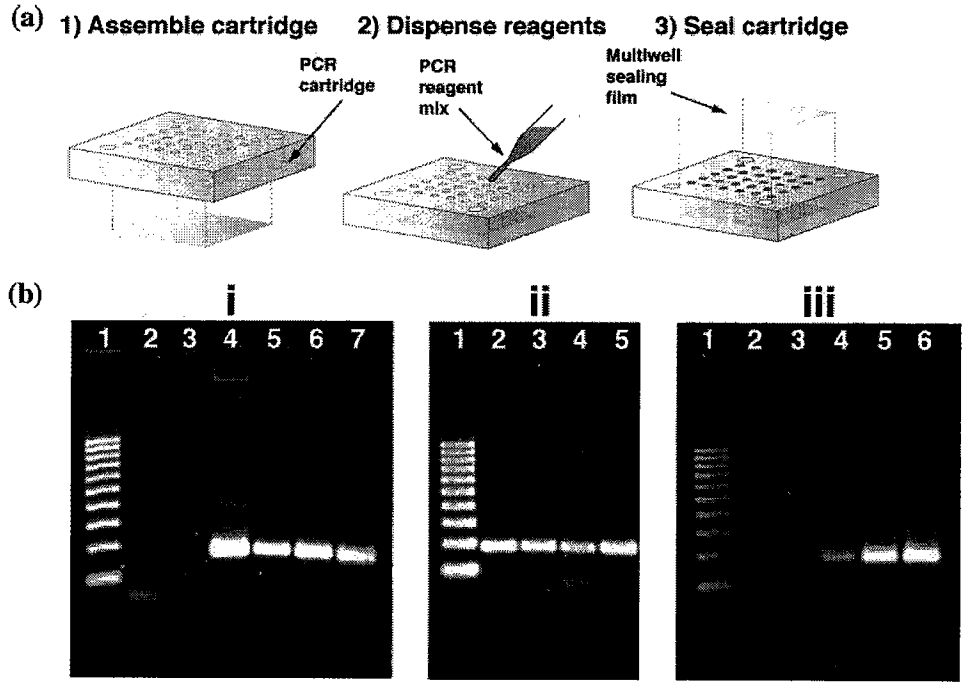

Figure 3. (a) Schematic illustration of the multiwell device assembly and loading process. Multiwell cartridges can be preloaded with a PCR master mix and stored under refrigeration for subsequent reactions. (b) PCR amplification of a 191-base pair fragment associated with membrane channel proteins M1 and M2 of the influenza-A virus using a cavity-based convective flow thermocycler. The top and bottom surfaces of PCR cartridge are maintained at 61 and 96 °C, respectively. (i) Comparison with conventional thermocycler (all reactions run in RB-PCR device for 40 min). Lane 1, 100-bp ladder; lane 2, negative control with no template; lane 3, negative control with no enzyme; lane 4, PCR product generated in a conventional thermocycler using a three-temperature cycling protocol (anneal, 61 °C; extend, 72 °C; denature, 95 °C; 35 cycles); lanes 5–7, PCR product from three parallel reactions in the multiwell convective flow device. (ii) Influence of initial template concentration (all reactions run in the convective flow device for 60 min). Lane 1, 100-bp ladder; lane 2, 5×10^5 copies; lane 3, 5×10^4 copies; lane 4, 5×10^3 copies; lane 5, 5×10^2 copies. (iii) Influence of reaction time in the convective flow device using a dilution of previous PCR product as template. Lane 1, 100-bp ladder; lane 2, negative control with no template; lane 3, negative control with no enzyme; lane 4, 15 min; lane 5, 20 min; lane 6, 30 min.

good agreement with those predicted in simulations (Figure 2). These in situ temperature and velocity characterization studies served to validate the ability of this simplified 2-D modeling approach to capture the essential features associated with the convective flow fields in high aspect ratio cavity systems.

To demonstrate the suitability of convective flow PCR systems for performing rapid biodetection assays, we used a multiwell cavity device to conduct a series of amplifications of a 191-base region associated with membrane channel proteins M1 and M2 of the influenza-A virus (Figure 3a). After 40 min of incubation in the convective flow device, levels of amplification comparable to those attainable in a conventional thermocycler (T-Gradient; Biometra) using a standard three-temperature cycling protocol (35 cycles, 2.5-h reaction time) could be routinely achieved (Figure 3b(i)). Typical product yields of 10 ng/μL were achieved in the convective flow device, as compared with 13 ng/μL in the thermocycler. No degradation in performance was observed over 4 orders of magnitude of initial template loading dilutions (Figure 3b(ii)), consistent with conventional thermocycler results. Amplification could be achieved in as little as 15 min when the original 3.9-kb template was replaced with a dilution of previous PCR product (Figure 3b(iii)). This level of speed is consistent with our expectations of the capabilities of convective flow-based thermocycling systems because individual fluid packets are able to establish thermal equilibrium with their surroundings almost instantaneously as they travel through spatial temperature zones within the reaction cavity. The accelerated reaction speed observed when using the 191-bp product as template is likely a consequence of a more rapid denaturing process relative to the longer 3.9-kb template fragment. These results illustrate the robustness of cavity-based convective flow PCR systems and demonstrate their ability to achieve performance equal to or exceeding conventional thermocycling hardware.

Thermocycling Using Convective Loops. One of the most powerful applications of buoyancy-driven natural convection in the context of biochemical analysis applications is the ability to spontaneously transport fluids through different spatial temperature zones simply in response to an applied temperature gradient. This behavior can be exploited to perform rapid thermocycling while simultaneously eliminating the need for dynamic external temperature control because (i) the convected fluid packets experience nearly instantaneous thermal equilibration with their surroundings as they travel through the flow network and (ii) the thermal mass to be heated and cooled consists entirely of the fluid actively involved in the reaction. This represents a significant departure from the vast majority of thermocycler designs ranging from benchtop instruments to microchips, most of which are characterized by relatively high time constants associated with the need to heat and cool additional "inactive" structural components.

Rectangular Loop Thermocyclers. In cavity-based convective flow systems, all reagents do not experience an identical thermal

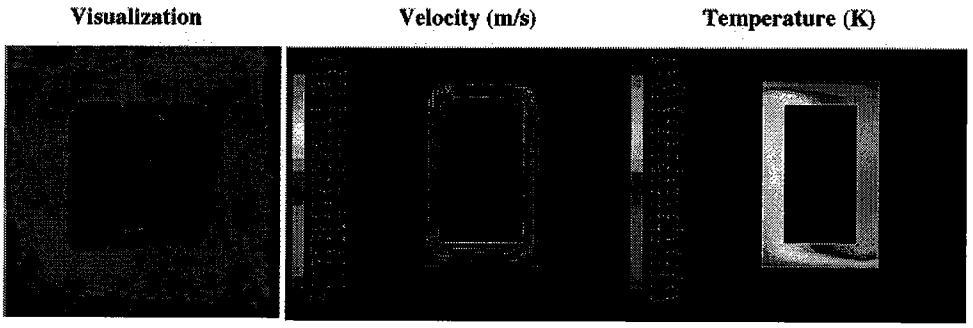

Figure 4. Flow visualization and simulation of the flow pattern within a rectangular loop structure heated from below. The photograph depicts the flow pattern in a rectangular loop 5 mm tall and 1.5 mm wide. The simulations show flow velocities and temperature profiles in 6-mm-tall and 750-μm-wide channels. Simulations were performed assuming adiabatic walls, and this is reflected in the temperature profiles depicted in the simulation. A movie of the convective motion is available online as Supporting Information.

history due to the spectrum of flow trajectories intrinsically present in the system. The use of closed-loop convection cells, however, allows specific thermal conditions to be maintained along sections of the flow path oriented orthogonally to the applied temperature gradient. Residence times within in each temperature zone can then be precisely determined by measuring the local velocity and controlled by adjusting the length and diameter of that section.

In the simplest case, a rectangular loop, a uniform vertical temperature gradient produces zones of constant temperature in the two horizontal segments of the loop, making the device well-suited for use in two-temperature cycling protocols (Figure 4). As is the case in macroscale symmetric torroidal flow loops, the direction or *handedness* of the fluid motion is determined by random perturbations and transient effects associated with initial application of the temperature gradient. Here, the handedness of the flow does not affect the net outcome of a thermocycling process because the symmetry of the flow loop ensures that the sequence in which the fluid is exposed to the various temperature zones is independent of flow direction. After experimenting with a variety of loop heights, we found that a favorable combination of thermal residence times and reaction temperatures in the horizontal segments of the loop could be achieved using loops 5–6 mm high, 4 mm wide, and ~700 μm in diameter. Corresponding flow simulations give reasonable velocity estimates and, when used in conjunction with flow visualization experiments, allow residence times in the denature (90 °C) and anneal/extend (60 °C) zones to be accurately predicted.

Flow visualization experiments indicate that the onset of convection in the loop occurs almost immediately upon application of a temperature gradient (accomplished by placing the device on the surface of a hotplate). A steady-state convective flow is established about 3–4 min after initial contact with the hot plate. These conditions (90 °C denature, 58 °C anneal/extend) yield average cycling times of ~20 s, although this could change during the course of an experiment as a few small air bubbles sometimes develop along the channel sidewalls. A schematic of the device used to demonstrate PCR amplification in a rectangular loop is shown in Figure 5a. PCR amplification performed by incubating the device on the hot plate for ~30 min yielded a band associated with the desired 295-bp product (Figure 5b). Two secondary bands and an intense low migrating band (not shown in photograph) consistent with formation of primer–dimer complexes are also present, possibly as a consequence of the relatively low denaturing

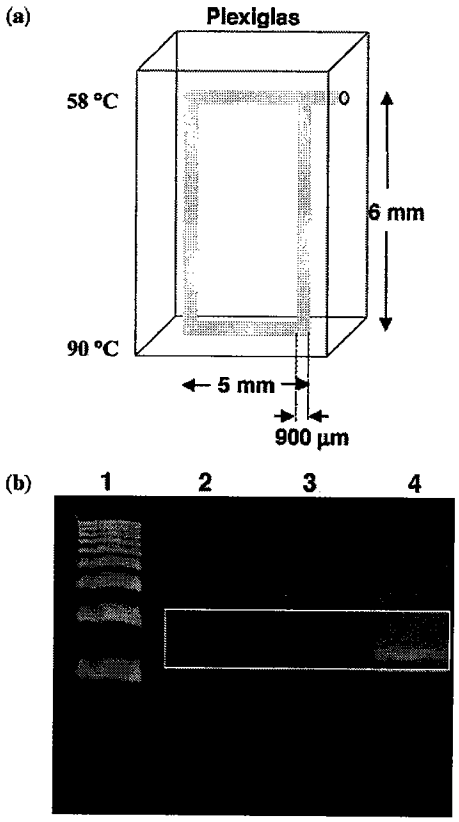

Figure 5. PCR in a rectangular flow loop. (a) Schematic representation of the Plexiglas device used to demonstrate PCR. (b) β-Actin PCR products generated with the convective loop structure compared with products generated in a conventional thermocycler (denature, 95 °C for 30 s; anneal/extend, 60 °C for 1 min; 40 cycles). Lane 1, 100-bp ladder; lane 2, PCR product from rectangular loop (15 μL loaded in gel); lanes 3 and 4, PCR products generated using the thermocycler (5 and 20 μL loaded in gel, respectively).

temperature employed. Comparison with the PCR product obtained by incubating an aliquot of the same reaction mixture in a conventional thermocycler shows a clear band at ~295 bp, but also exhibits considerable background smearing compared to the loop PCR product.

The feasibility of performing PCR amplification in a convective loop format is further illustrated by constructing a series of closed-

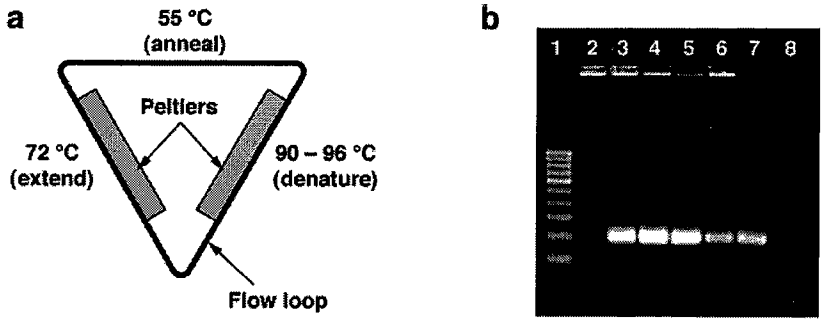

Figure 6. (a) Schematic illustration of a 15-μL closed-loop convective flow thermocycler constructed using inexpensive fluoropolymer tubing and Peltier heating elements. The flow direction is counterclockwise. (b) Series of amplification reactions evaluating the effect of temperature maintained in the denaturing segment of the flow loop. The reagent mixture employed was identical to that used to obtain the data in Figure 3b (3.9-kb template size). Lane 1, 100-bp ladder; lane 2, 96 °C denaturing temperature; lane 3, 95 °C; lane 4, 94 °C; lane 5, 93 °C; lane 6, 92 °C; lane 7, 91 °C; lane 8, 90 °C.

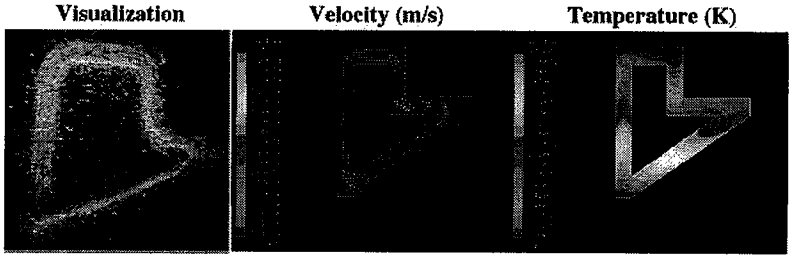

Figure 7. Flow visualization and simulation of the flow pattern within a "three-temperature loop" structure heated from below. The photograph depicts flow trajectories in a loop that is 6 mm tall and constructed using 700-μm-wide channels, except for the oblique bottom section of the loop which is 300 μm wide (volume ~7 μL). The simulations depict flow profiles and temperatures in 6-mm-tall loops of uniform thickness. A vertical temperature gradient was imposed on all vertical walls of the loop, with constant-temperature boundary conditions imposed along the horizontal walls. A movie of the convective motion is available online as Supporting Information.

flow circuits using fluoropolymer tubing. Lengths of tubing incorporating 15-μL reaction volumes were filled with a PCR reagent mixture, sealed, and wrapped around a fixture designed to create a triangular flow path in which the horizontally opposed arms were maintained at denaturing and extension temperatures using independently controlled Peltier heaters (Figure 6a). Flow visualization experiments using fluorescent microspheres indicated that velocities on the order of 0.7 mm/s were achieved under these conditions, corresponding to a cycle time of ~2.25 min. When the flow loop was loaded with PCR reagents, a successful 40-cycle amplification of the 191-base pair fragment (3.9-kb template size) could be performed in 90 min with results comparable to conventional thermocyclers (Figure 6b). It is notable that no modifications to the reagent mixtures (e.g., surface passivation additives) used in conventional thermocycler-based protocols were necessary in either the cavity- or loop-based PCR devices presented here. Further optimization of the flow field and scale-down of the reactor volume are likely to yield improved cycling performance.

Three-Temperature Asymmetric Flow Loops. The capability to support three-temperature cycling protocols is desirable in order for a thermocycler to be truly flexible and compatible with virtually any PCR amplification biochemistry. We addressed this issue by constructing convective flow loops heated from below incorporating two horizontal segments with a V-shaped "bend zone" at the bottom of the loop to provide three distinct temperature regions (Figure 7). The overall height of the structure was ~6 mm and the flow channels incorporated thick (700-μm-diameter) and thin (300-μm-diameter) sections.

Most flow loop structures we have described thus far possess symmetry about the vertical axis, so that the handedness of the flow though the loop is of no practical concern. The situation is different in these vertically asymmetric flow loops, where the handedness of flow though the loop needs to be controlled so that fluid motion will proceed only in the direction producing cyclic exposure to the appropriate reaction temperatures *in the proper order*, irrespective of the initial perturbations and nonidealities present in the system. In experiments using three-temperature-zone flow loops of uniform thickness, we found that fluid motion often occurred in the direction opposite to the required temperature sequence. On rare occasions, a flow of the desired handedness developed, but this was not reproducible and was attributed to random perturbations associated with those particular experiments. By modifying the geometry in localized sections of the loop, however, we found that the flow could be biased to move in the direction of the desired handedness. This biasing effect appears to exhibit a sensitive dependence on the detailed geometry of the flow loop. It is also possible to control the handedness of the flow by superimposing a weak horizontal temperature gradient, so that the loop is preferentially heated along the vertical edge of one side causing upward fluid motion to occur in the vertical limb closest to the heater. Another possibility for controlling the handedness of flow, particularly in microfabricated systems, is to use heaters positioned at specific locations along the loop perimeter to induce thermal perturbations that initiate and bias the flow direction.

Control of Residence Time in Convection Loops. Most PCR cycling protocols are designed to expose the fluid to denaturing

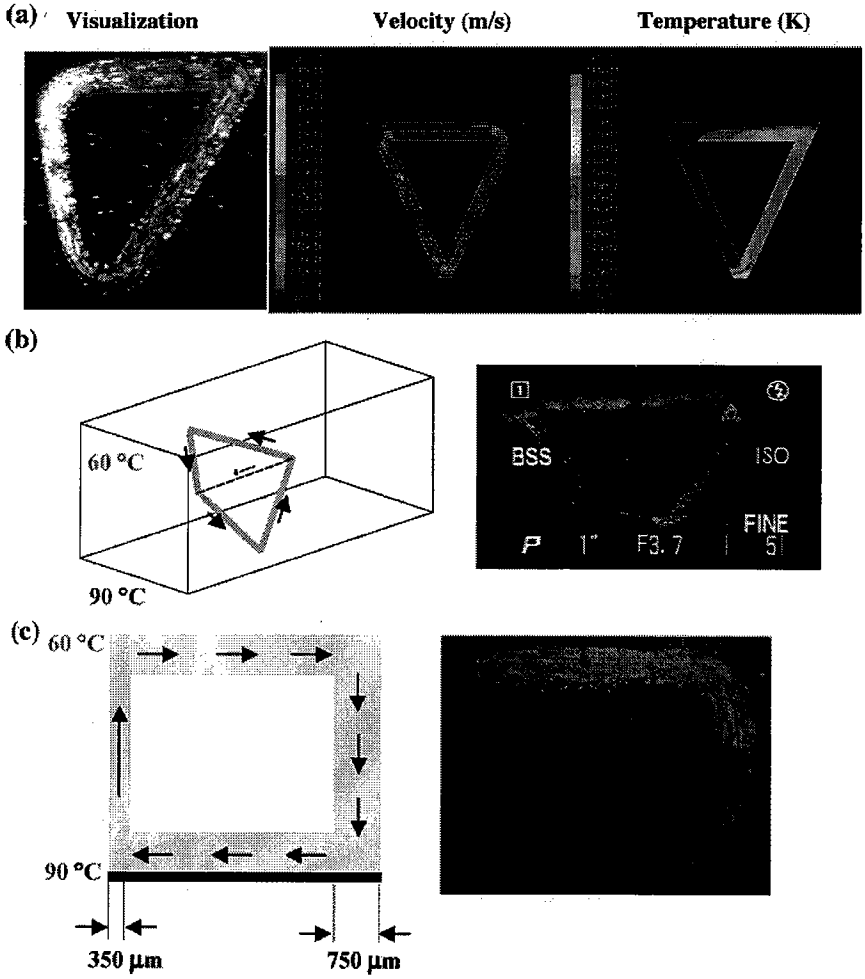

Figure 8. Strategies for controlling thermal residence times within convective loops. (a) Flow visualization and simulation of a triangular loop structure heated from below. The loop was 6 mm tall and 750 μm wide, and the simulations were performed assuming adiabatic walls. The triangular structure results in a shorter residence time within the denaturing section of the loop. (b) Modification of the triangular loop structure incorporating a 3-D V-shaped top section to produce longer residence times at the anneal/extend temperature. The device was heated from below, and fluid flow velocities of the order of a few millimeters per second were observed within the loop. (c) Rectangular loop structure modified to include a vertical limb of reduced cross section. The structure was heated from below and the fluid velocity in the narrow limb was found to be higher than that in the rest of the loop, thereby providing a means of controlling thermal residence times during thermocycling. Movies of the convective motion in (a–c) are available online as Supporting Information.

conditions only very briefly because the process is practically instantaneous and because protracted exposure to high temperatures gradually degrades performance of many *Taq* polymerase enzymes. This condition can be satisfied in a convective flow system through the use of a triangular loop design, where one apex of the triangle is located at the bottom of the flow path (maximum temperature) while the opposite side is located at the top of the loop (anneal/extend temperature). When heated from below, the residence time within the denaturing section can be minimized resulting in a corresponding reduction in overall cycling time (Figure 8a).

The triangular loop design can be further modified by incorporating a 3-D segment that allows the fluid to traverse a longer path in the horizontal plane within the anneal/extend zone. Such a structure is shown in Figure 8b where the longer path forms a "V" protruding into the plane of the paper. Consequently, the residence time within anneal/extend temperature conditions can be increased without varying any global geometric parameters such as the height or diameter of the flow loop. Additional control over heating and cooling rates within a given flow loop can be achieved by adjusting the diameter of the vertical limbs connecting the two horizontal temperature zones, resulting in a proportionate increase in fluid velocity within these regions (Figure 8c). These simple modifications permit a considerable degree of versatility in the design of tunable convective flow thermocyclers.

Convective Flows in Miniaturized Systems. This type of convectively driven circulation can also be used to mix liquid droplets in microfluidic channel structures. Mixing of liquids in microchannels has received considerable attention in the literature on miniaturized analysis systems. This is primarily due to the fact that diffusion is the only available mechanism to achieve mixing in the laminar flow regime and that droplet lengths are usually large enough to make axial mixing time scales prohibitively long. By incorporating a simple geometric modification to a microfluidic channel and applying a temperature gradient, rapid convectively driven axial mixing can be induced along the entire length of a

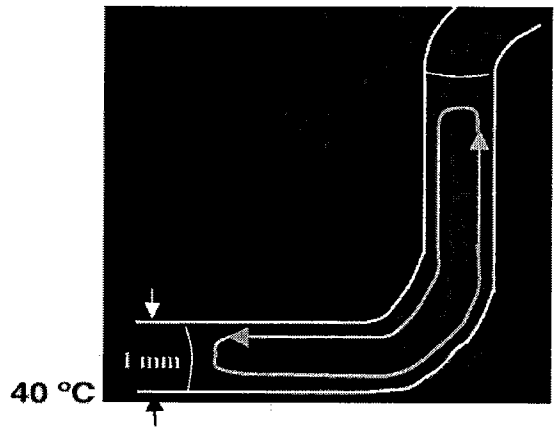

Figure 9. Photograph of mixing in a microfluidic channel using natural convection. The arrows indicate the recirculation pattern observed upon raising the temperature at the bottom of the elastomeric device to 40 °C. A movie of the convective motion is available online as Supporting Information.

droplet. To demonstrate this, a thermoplastic elastomer substrate was used to construct such a mixer (Figure 9). Here, a droplet almost 1 cm in length containing an aqueous solution of 6-μm-diameter fluorescent latex microspheres was injected into a 1-mm-diameter channel of circular cross section. The droplet was then positioned such that the horizontal edge of the flow channel bend was in contact with a hot plate set at 40 °C. Circulatory flow patterns generated within the droplet are capable of performing mixing as a consequence of continual expansion of the interfacial area between parallel streamlines. This action is analogous to that observed in moving droplets and characterized by Handique and Burns.[20]

We have demonstrated continuous unidirectional nonpulsatile flows in a variety of loop geometries, sizes, and diameters in melt-processable thermoplastic elastomer substrates. For instance, a horizontal temperature gradient was imposed by placing a thermoelectric (Peltier) heater in contact with one side of the device while the other side remained exposed to the ambient air (Figure 10a). Flow velocities were determined by recording the motion of an aqueous suspension of 6-μm-diameter fluorescent latex microspheres, and temperature gradients were measured using thermocouple probes inserted near both vertical segments of the flow loop. We observed that the onset of fluid motion occurred in response to the application of a very small temperature difference between the two vertical segments of the loop (on the order of 1 °C or less), consistent with the low value of Ra_{crit} in this system. As the magnitude of the horizontal temperature gradient imposed across the loop is increased, the flow rate generated inside the loop also increases in a manner that scales with Ra/Pr, where Pr is the Prandtl number (ν/κ) and Ra is computed using eq 2 (Figure 11a). The dependence of flow rate on the magnitude of the horizontal temperature gradient imposed across the loop, in channels of various diameters, is shown in Figure 11b.

The length scales associated with these convective flow loops are ideally suited for the construction of low-power miniaturized thermocycling devices in plastic substrates. Both the Plexiglas substrate used to construct convective flow PCR devices and the

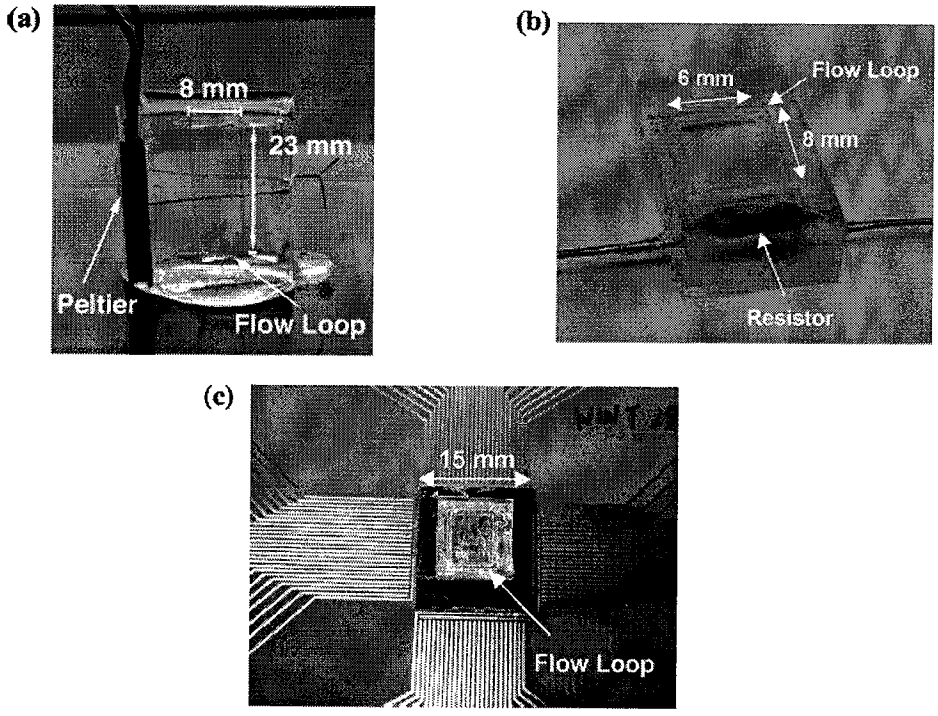

Figure 10. Photographs of prototype convective flow devices. (a) A loop device constructed using a melt-processable thermoplastic elastomer substrate. A horizontal temperature gradient was imposed by placing a thermoelectric (Peltier) heater in contact with one side of the device while the other side remained exposed to the ambient air. (b) A Plexiglas device using an ordinary 1-Ω resistor as a constant-temperature heater. Actuation of the heater imposes a vertical temperature gradient through the Plexiglas structure sufficient to generate convective flow through the loop. (c) A silicon–polymer hybrid structure incorporating an array of microfabricated heaters and temperature sensors on the silicon side that can be selectively used to heat specific locations of the flow.

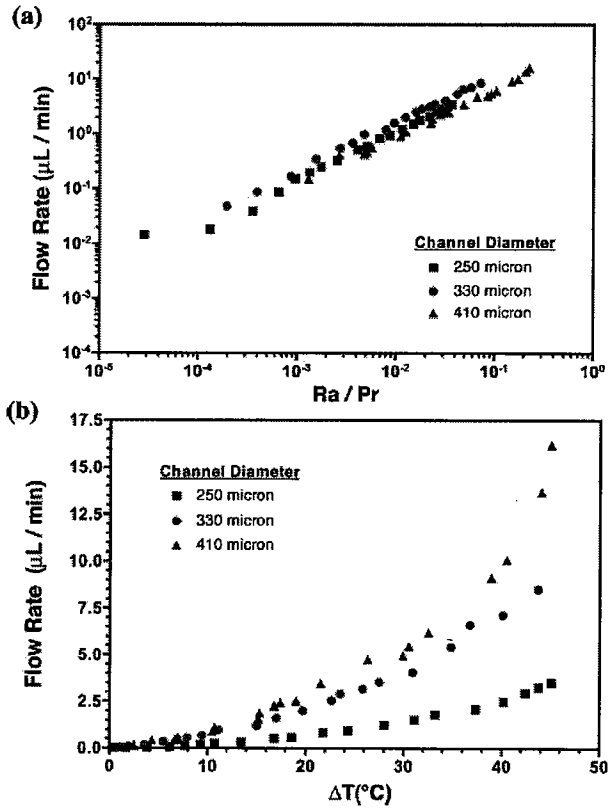

Figure 11. (a) Scaling of flow rate data measured in the convective flow device shown in Figure 10a with *Ra/Pr*. (b) Dependence of pumping capacity on flow channel diameter.

thermoplastic elastomer employed in the investigations of flow fields in various loop geometries are capable of sustaining relatively high-temperature gradients. More importantly, we found that when these devices were placed on the surface of a constant-temperature hot plate to maintain the bottom of the loop at 90 °C, the uppermost arm of the 6-mm-tall loop structures naturally experienced temperatures in the vicinity of 58 °C solely through exposure to the ambient air. This observation suggests that convective flow PCR devices can be constructed using only a single built-in constant-temperature heater, either externally assembled or integrated into the device using microfabrication techniques.

A 2-D MATLAB simulation of the steady-state temperature profile in a Plexiglas device incorporating a 200-μm gold resistive heating element shows that the temperature profile required to run PCR in the flow loop can be generated with a power consumption as low as 60 mW—well within the capabilities of conventional batteries. To illustrate this point, we constructed a prototype device incorporating an additional access channel 3 mm in diameter in proximity to the lower limb of a rectangular Plexiglas flow loop ($h = 6$ mm, $d = 900$ μm). A 1-Ω resistor was inserted through this channel to simulate the function of a metallic resistive heating element in a microfabricated device. The resistor was centered beneath the lower limb of the loop and held in place using silicone gel to ensure uniform thermal contact with the body of the Plexiglas structure (Figure 10b). Even using this crude design, a convective flow field with fluid velocities on the order of millimeters per second could be generated in the loop with power consumption in the vicinity of 360 mW. The discrepancy between actual and predicted power consumption is attributable to the finite thickness of the prototype device not captured in the 2-D simulation and losses associated with the contact nonidealities between the resistor and the Plexiglas body of the device.

While the Plexiglas prototype using an ordinary resistor as a heating element illustrates the feasibility of building portable low-power PCR devices in a miniaturized "chip" format, the availability of only a single heating element on one side of the loop structure limits its flexibility. To further enhance the versatility of loop flows and the adaptability of loop structures to flow control in microfabricated systems, we bonded a loop structure molded from thermoplastic elastomer material to the surface of a microfabricated silicon substrate patterned with an array of heaters and temperature sensors (Figure 10c). The flow loop incorporated a channel diameter of 750 μm with a loop height of 6 mm, and the silicon device occupied a footprint of approximately 1.5 cm × 1.5 cm. The elastomer created an instantaneous seal to the oxide surface of the die, ensuring good thermal contact. When a specific heater located in the lower right-hand corner of the chip was actuated, a convective flow field with fluid velocities of the order millimeters per second was immediately established inside the loop. This initial device design allowed temperatures of 40 and 30 °C to be established along the bottom and top surfaces of the device, respectively. Higher temperature gradients can be readily achieved through proper thermal isolation or the use of polymeric substrate materials. Such devices can be easily and inexpensively mass-produced using conventional micromachining techniques.

A few general guidelines for the scale-down of convective flow systems in cavities and miniaturized loops can be derived. For cavity systems, an estimate of the minimum reactor volumes available can be obtained by recognizing that the minimum flow velocity will occur in the vicinity of the critical Rayleigh number. The scaling $Ra_{crit} = 1087(h/d)^4$ can then be evaluated as a function of h/d to extract the minimum allowable reactor volume corresponding to a given aspect ratio. The results of this analysis (assuming thermal properties of water at 80 °C) indicate that reactor volumes ranging from 230 nL ($h/d = 1$) to 200 μL ($h/d = 30$) are achievable in cavity-based systems. For loop-based devices, we can use the flow rate data in Figure 11b to extract a rough estimate of the minimum channel diameter for flow to occur by extrapolating to the conditions corresponding to zero flow rate. This analysis indicates that channel diameters can be scaled down to at least 180 μm at this tubing diameter (28 gauge), maintaining a temperature difference of 35 °C between annealing and denaturing temperatures. This minimum diameter can be further reduced through the use of shorter flow loops because the corresponding decrease in hydrodynamic resistance allows higher flow rates to be achieved under the same thermal driving force.

CONCLUSIONS

In this paper, we demonstrate the power and incredible versatility of natural convection in analytical fluidic operations and an entirely new adaptations in the area of miniaturized systems. Our results illustrate the robustness of cavity-based convective flow PCR systems and demonstrate their ability to achieve

(20) Handique, K.; Burns, M. A. *J. Micromechan. Microeng.* **2001**, *11*, 548–554.

performance comparable to conventional thermocycling hardware in a rapid and inexpensive format. PCR cartridges incorporating a variety of layouts (e.g., conventional 96- or 384-well microplate formats) can be easily produced at minimal cost, making it feasible for them to be disposable. Multiple geometries can also be incorporated within the same cartridge to simultaneously perform reactions involving different thermal cycling profiles. While it is true that different reactor cartridges would be required in order to tailor cycling parameters in a cavity-based system, it is unlikely that this would impose a severe limitation on the ability to accommodate different reaction parameters. Based on our experience, we find that a given reactor geometry is effective over at least a 5−7 °C range of annealing temperatures. This implies that a fixed set of three to five "universal" reactor cartridges would be sufficient to meet the needs of the majority of thermocycling profiles.

Loop-based convective flow microdevices are capable of achieving mixing, pumping, and thermocycling for PCR using a greatly simplified hardware format. We found that convection in closed loops provides an ideal platform for PCR, as demonstrated by successful amplification with a 2-fold reduction in reaction volume compared to our previously reported studies in cylindrical cavities. Our experiments on mixing and pumping used gradients established by elevating the temperature on one side of the flow loop. These phenomena, however, depend on the *temperature difference* applied across the channel network rather than absolute temperature magnitudes, and our choice was motivated purely by experimental simplicity. In miniaturized systems employing temperature-sensitive fluid samples (e.g., enzymes), similar flows can be generated using cooling rather than heating to induce the necessary temperature gradients, thereby avoiding the possibility of sample degradation at elevated temperatures. Although convective loops must be carefully loaded to ensure that bubble formation will not block the flow, the ease with which they can be constructed with ordinary tubing offers an attractive format for integration with downstream capillary-based analytical processes (e.g. capillary electrophoresis).

One of the most critical issues in the design of any new thermocycling technology is evaluating its performance relative to existing hardware. The primary advantages of the RB-PCR system over conventional technology are (i) a hardware design that is simple and inexpensive to produce, (ii) faster reaction speeds (up to 10 times faster), and (iii) flexibility to incorporate a wide range of reactor volumes and geometries to integrate with existing laboratory protocols and liquid handling systems. In terms of speed, we have achieved reaction times as short as 15 min in our current cavity systems using 30-μL volumes (Figure 3). We expect reaction times on the order of 10 min or less to be reasonably achievable through the use of smaller reaction volumes and further optimization of the flow field. Our current loop designs deliver cycling times ranging from 15 to 20 s to 2 min per cycle using reactor volumes on the order of 15 μL.

The inherent simplicity of natural convection-driven thermocycling also offers compelling advantages over current microchip-based thermocycler designs. In addition to all the benefits of scaling down (e.g., faster heating and cooling rates, reduced reagent consumption), these devices completely eliminate the electronic control component necessary to perform dynamic temperature cycling. Though traditional PCR microchips have achieved a significant reduction in process time compared to their macroscopic counterparts (on the order of 15−30 s/cycle[21,22]), their speed of operation is still limited by the heating and cooling rates of the hardware components used to construct the microreactor. The convection-based thermocyclers described here drive the reaction by establishing a steady-state temperature gradient through the substrate, eliminating the inherent heating and cooling time constants and power loss associated with traditional thermocycling devices, and providing the opportunity to perform PCR at speeds limited solely by the kinetics of the reaction.

ACKNOWLEDGMENT

We gratefully acknowledge Slava Berejnov for helpful discussions regarding convective flow loops, Ana Ugaz for assistance with PCR in the multiwell cavity system, and Kalee D. Spitzack for assistance with quantification of product yields. This work was supported by the National Institutes of Health under Grants NIH R01-HB01044 (M.A.B.), NIH R01-HG01046 (M.A.B.), and NIH K22-HG02297 (V.M.U.).

SUPPORTING INFORMATION AVAILABLE

Additional information as noted in text. This material is available free of charge via the Internet at http://pubs.acs.org.

Received for review May 7, 2004. Accepted August 19, 2004.

AC049323U

(21) Belgrader P.; Benett W.; Hadley D.; Richards J.; Stratton P.; Mariella R.; Milanovich F. *Science* **1999**, *284*, 449−450.

(22) Lagally E. T.; Medintz I.; Mathies R. A. *Anal. Chem.* **2001**, *73*, 565−570.